INSTITUTE OF PHYSICS PUBLISHING JOURNAL OF PHYSICS B: ATOMIC, MOLECULAR AND OPTICAL PHYSICS

J. Phys. B: At. Mol. Opt. Phys. **36** (2003) L25–L30 PII: S0953-4075(03)54880-5

LETTER TO THE EDITOR

Carbon K-shell photoelectron angular distribution from fixed-in-space CO_2 molecules

N Saito[1], A De Fanis[2], K Kubozuka[3], M Machida[3], M Takahashi[2], H Yoshida[4], I H Suzuki[1], A Cassimi[5], A Czasch[6], L Schmidt[6], R Dörner[6], K Wang[7], B Zimmermann[7], V McKoy[7], I Koyano[3] and K Ueda[2,8]

[1] National Metrology Institute of Japan, AIST, Tsukuba 305-8568, Japan
[2] Institute of Multidisciplinary Research for Advanced Materials, Tohoku University, Sendai 980-8577, Japan
[3] Department of Material Science, Himeji Institute of Technology, Kamigori, Hyogo 678-1297, Japan
[4] Department of Physical Science, Hiroshima University, Higashi-Hiroshima 739-8526, Japan
[5] CIRIL/CEA/CNRS/ISMRA, Université de Caen, Box 5133, F-14070 Caen Cedex 5, France
[6] Institut für Kernphysik, Universität Frankfurt, D-60486 Frankfurt, Germany
[7] A A Noyes Laboratory of Chemical Physics, California Institute of Technology, Pasadena, CA 91125, USA

E-mail: ueda@tagen.tohoku.ac.jp

Received 7 October 2002
Published 20 December 2002
Online at stacks.iop.org/JPhysB/36/L25

Abstract

Measurements of photoelectron angular distributions for carbon K-shell ionization of fixed-in-space CO_2 molecules with the molecular axis oriented along, perpendicular and at 45° to the electric vector of the light are reported. The major features of these measured spectra are fairly well reproduced by calculations employing a relaxed-core Hartree–Fock approach. In contrast to the angular distribution for K-shell ionization of N_2, which exhibits a rich structure dominated by the f-wave ($l = 3$) at the shape resonance, the angular distribution for carbon K-shell photoionization of CO_2 is quite unstructured over the entire observed range across the shape resonance.

(Some figures in this article are in colour only in the electronic version)

There have been significant advances in the development of techniques for measuring angular distributions of photoelectrons from fixed-in-space molecules (see, for example, [1–3]). To date these techniques have been extensively used to study the angular distributions of K-shell photoelectrons emitted from the diatomics CO and N_2 (see, for example, [1–7]). The measurements have confirmed the rich dynamical structure of photoelectron angular distributions for fixed-in-space molecules predicted in the seminal studies of Dehmer and

[8] Author to whom any correspondence should be addressed.

Dill some 25 years ago [8]. These distributions have been particularly insightful in regions of shape resonances for K-shell photoelectrons from small molecules where they provide a dynamical window on the underlying partial-wave composition of the photoelectron as it scatters off the anisotropic potential of the ion. Furthermore, recent calculations employing Hartree–Fock and random-phase-approximation methods and an extension of the standard multiple scattering approach have yielded angular distributions which reproduce key features of the measured spectra quite well [4, 7, 9]. It is clearly of interest to extend these measurements and calculations to triatomic molecules in order to explore any dynamical features that may arise in these photoelectron angular distributions for systems beyond simple diatomics such as CO and N_2. Oxygen K-shell photoelectron distributions from fixed-in-space CO_2 have been previously reported but only for the molecular axis parallel to the polarization vector of the light [10]. In this letter we report results of measurements and calculations for carbon K-shell photoelectrons for fixed-in-space CO_2 molecules across the shape resonance around 312 eV.

The experimental technique employed in this study is electron–ion coincidence momentum imaging. A supersonic jet of CO_2 crosses a beam of linearly polarized radiation at right angles in the ionization region of the time-of-flight (TOF) spectrometer. The axis of the spectrometer is perpendicular to both the gas and photon beams. Ions are accelerated by a uniform electrostatic field to a micro-channel-plate (MCP) detector at one end of the acceleration region while the field accelerates electrons to the other side where they enter the drift region. The lengths of the electron acceleration and drift regions are 70 and 140 mm, respectively, satisfying the Wiley–McLaren space-focusing condition [11]. A uniform magnetic field helps drive the electrons toward the MCP detector at the end of the drift region. Each MCP detector is fitted to a two-dimensional (2D) multi-hit readout delay-time anode (RD-80 for ions and HEX-80 for electrons) manufactured by Roentdek [12]. This permits measurements of both the time of detection and their 2D position coordinates. The momentum component of the particle along the axis of the spectrometer can be extracted from the TOF measurements which, together with the position of detection data, also permit extraction of the other two momentum components in a plane perpendicular to the axis of the spectrometer.

The measurements were carried out on the *c* branch of the figure 8 undulator beamline 27SU at SPring-8 in Japan [13–15], using the several-single-bunches mode of operation of the storage ring. The 10 single-bunches + 1/12 and 18 single-bunches + 2/21 filling modes employed in the present studies provide bunch intervals of 399.2 and 228.1 ns, respectively, and permit electron TOF measurements. Appropriate tuning gates select only those electron signals synchronized with the single bunches and the TOF spectra of the electrons are measured with respect to the bunch marker of the synchrotron radiation source. We record only events in which at least two ions and one electron are detected in coincidence. The orientation of the molecular axis at the moment of photoionization is extracted from the momentum vectors of the CO^+ and O^+ fragments, resulting from Coulomb dissociation of CO_2^{2+} subsequent to rapid Auger decay. Coincidence measurements were recorded at energies shown by vertical bars in figure 1, where an electron yield spectrum in the region of the $C(1s^{-1})$ ionization threshold [16] is presented. The $C(1s^{-1})$ ionization threshold at 297.63 eV [17] is also marked in figure 1.

Our calculated photoelectron angular distributions were obtained within a relaxed-core Hartree–Fock (RCHF) approximation with a molecular basis set obtained using Slater's transition state approximation [9, 18]. In this approximation the relaxed molecular orbitals are derived from a self-consistent calculation where half an electron is removed from the carbon K-shell. This procedure attempts to capture effects arising from screening of the K-shell hole while maintaining the calculation at the one-electron level. To avoid working with non-orthogonal orbitals we also use this molecular basis to construct the initial N-electron state and the final N-electron state with an electron in the continuum [9]. To obtain the photoelectron

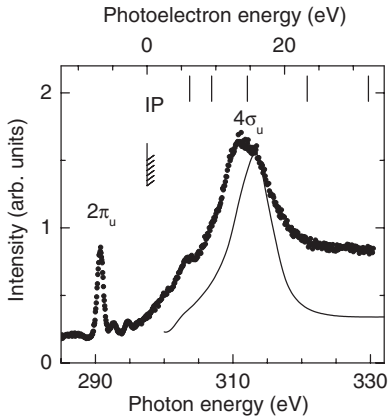

Figure 1. Electron yield spectrum of CO_2 in the energy region of the $C(1s^{-1})$ ionization threshold reported by Bozek *et al* [16]. The marks indicate the energies where the photoelectron angular distributions have been measured in coincidence with ions. The full curve indicates the C 1s photoionization cross section calculated within a RCHF approximation using Slater's transition state approximation.

orbitals we used an iterative procedure to solve the Lippmann–Schwinger equation associated with the one-electron Schrödinger equation with a potential produced by the *transition-state* orbitals. The calculated C 1s photoionization spectrum is compared with the measured electron yield spectrum in figure 1 (from [16]) and shows that this potential reproduces the peak position of the shape resonance well.

Figure 2 shows our measured (dots) and calculated (curves) angular distributions for photoelectrons emitted from the carbon K-shell of fixed-in-space CO_2 at electron kinetic energies of 6.2, 9.4, 14.6, 23.3 and 32.2 eV. The electric vector of the light is horizontal and orientations of the molecular axis are 0°, 45° and 90° with respect to the electric vector. The distributions for molecular orientations of 0° and 90° correspond to $\Sigma \rightarrow \Sigma$ (referred to as Σ) and $\Sigma \rightarrow \Pi(\Pi)$ transitions, respectively. For better comparison with the measured data, the calculated distributions in figure 2 have been convoluted with a Gaussian distribution with a FWHM of 15°, corresponding to the experimental angular resolution. The distribution at each energy is normalized so that the integrated intensity (area enclosed) for the Σ channel is unity for both the measured and calculated spectra. The distributions for different orientations of the molecular axis (0°, 45° and 90°) are on relative scales. The Σ channel is particularly strong at kinetic energies of 9.4 and 14.6 eV and thus the corresponding data for 45° and 90° are multiplied by a factor of 2 or 4, as indicated in the figure.

Note that the experiment resolves O^+ and CO^+ fragments and hence the measured photoelectron distributions need not display reflection symmetry through a plane perpendicular to the molecular axis, if the photoemission is related to asymmetric O^+–CO^+ fragmentation. The measured photoelectron distributions do, however, show this symmetry for the Σ and Π channels and we take this to be an indication that electron emission is independent of asymmetric molecular fragmentation. The calculated photoelectron distributions, which are generally in quantitative agreement with the measured spectra, were obtained in $D_{\infty h}$ symmetry.

We first focus on the angular distributions in the Σ channel where the electric vector is parallel to the molecular axis. In this channel only odd partial wave components of the dipole matrix element arise in photoionization of the σ_g (C(1s)) orbital. The partial wave composition ($l = 1$, 3, 5 and 7) of the photoionization amplitudes can provide useful insight

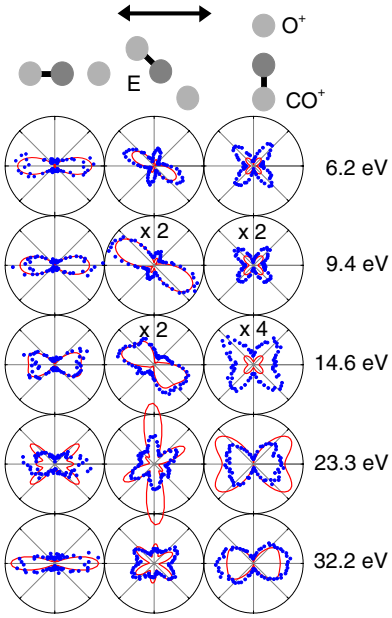

Figure 2. C 1s photoelectron angular distributions from fixed-in-space CO_2 molecules at electron kinetic energies of 6.2, 9.4, 14.6, 23.3 and 32.2 eV. The dots and curves correspond to measurements and calculations, respectively. The direction of polarization, E, is horizontal. The molecular axis is at 0°, 45° and 90° with respect to E.

into the angular distributions in this channel. Figure 3 shows these amplitudes as well as their real and imaginary components. In addition to a substantial p ($l = 1$) component expected for ionization of a σ_g (C (1s)) orbital, higher l (3 and 5) contributions are seen to be significant, not only at the shape resonance around an electron energy of ∼14 eV, but also at lower and higher photoelectron energies. The calculated angular distributions in figure 2 reproduce the general features of the measured spectra reasonably well except at an electron energy of 23.3 eV where the calculated cross section exhibits sharper structure than may be apparent in the experimental data. The distributions at lower energies of 6.2 and 9.4 eV, ∼8 and 5 eV below the peak of the shape resonance, respectively, are more peaked along the electric vector than would be expected for the pure p-wave. This behaviour very likely arises from interference between the $l = 1$ and 3 waves. At an energy of 14.6 eV in the peak region of the resonance, the angular distribution is not as peaked along the molecular axis as those at lower energies and reflects interference among the $l = 1$, 3 and 5 waves, which are all quite significant around 14 eV. It is worth noting that this behaviour is in sharp contrast with the distribution in the diatomic molecule N_2 where a rich structure dominated by a single $l(=3)$ is seen.

Agreement between the calculated and measured angular distributions at an electron energy of 23.3 eV in the Σ channel is clearly less satisfactory than at the lower energies in figure 2. The calculated distribution displays sharp structure which is not apparent in the measured spectra. This disagreement may be due to neglect of vibrational motion in the calculated spectra, which were obtained at the ground state geometry. Finally, the calculated and measured angular distributions at the highest photoelectron energy studied here is quite good.

In the Π channel, where the electric vector is perpendicular to the molecular axis and no shape resonance is seen, the shapes of the calculated and measured angular distributions are

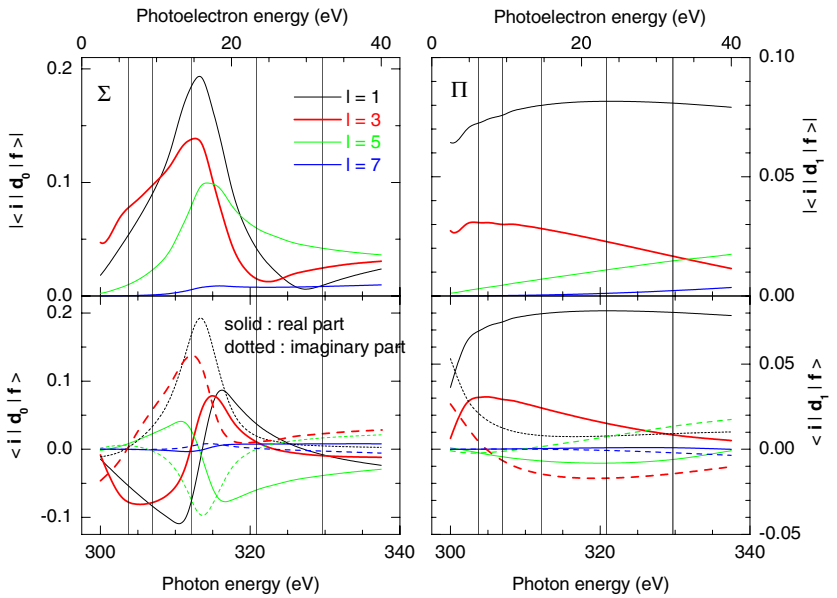

Figure 3. Amplitudes, as well as real and imaginary parts, of the dipole moments for the partial waves $l = 1$, 3, 5 and 7 for the Σ and Π channels, calculated within a RCHF approximation using Slater's transition state approximation. Vertical lines indicate the energies where the photoelectron angular distributions from fixed-in-space CO_2 have been measured and calculated.

in good agreement at the five energies shown in figure 3. The calculated intensities, however, are clearly lower than the measured ones at the lower energies of 6.2, 9.4 and 14.6 eV. This is due to our normalization of the intensities of the calculated and measured distributions in the Σ channel and an overestimation of the calculated intensities in the shape resonance region of the Σ channel. At lower energies electron emission along the electric vector of light is less pronounced than at higher energies and exhibits structure characteristic of an $l = 2$ wave, which is forbidden in this channel. As the energy increases electron emission along the electron vector becomes more pronounced.

Figure 2 also shows measured and calculated angular distributions for an orientation of 45° between the electric vector and molecular axis. These distributions are determined by a coherent mixture of the Σ and Π channels and both the ratios of amplitudes and phases in these channels play a significant role. These distributions can hence be additional benchmarks for testing theoretical methods and models. Agreement between the calculated and measured distributions is quite reasonable and suggests that the calculated phase relationship between the Σ and Π channels is satisfactory. The underestimation of the intensities of the minor lobes at the lower energies of 6.2 and 9.4 eV is again probably due to an overestimation of the intensity of the Σ channel relative to the Π, as discussed above.

In conclusion, we have reported on the results of measurements and calculations of photoelectron angular distributions for fixed-in-space CO_2 in the carbon K-shell region not only for the Σ and Π channels, where the molecular axis is parallel and perpendicular to the electric vector, but also for the molecular axis oriented at 45° to the electric vector. In contrast to the angular distribution in the resonance region for K-shell ionization of the diatomic molecule N_2, which exhibits a rich structure dominated by the $l = 3$ wave, both the calculated and measured distributions at resonance for the carbon K-shell of CO_2 are quite unstructured. This behaviour

is attributed to interference among dominant partial waves. Though agreement between the measured and calculated distributions is, on average, reasonable, the calculated distribution at an electron energy of 23.3 eV displays a structure which is not apparent in the measurement.

The measurements were carried out with approval of the SPring-8 Programme Advisory Committee and supported in part by Grants-in-Aid for Scientific Research from the Japan Society for the Promotion of Science and by the Matsuo Foundation. The authors are grateful to the staff of SPring-8 for their help in the course of these studies. LS, RD and AC acknowledge support by DFG. AD acknowledges financial support from the Japan Society for the Promotion of Science (JSPS). BZ would like to thank the Alexander von Humboldt Foundation (Germany) for the Feodor Lynen Research award.

References

[1] Shigemasa E, Adachi J, Oura M and Yagishita A 1995 *Phys. Rev. Lett.* **74** 359
[2] Heiser F, Gesner G, Viefhaus J, Wieliczek K, Hentges R and Becker U 1997 *Phys. Rev. Lett.* **79** 2435
[3] Landers A *et al* 2001 *Phys. Rev. Lett.* **87** 013002
[4] Cherepkov N A, Semenov S K, Hikosaka Y, Ito K, Motoki S and Yagishita A 2000 *Phys. Rev. Lett.* **84** 250
[5] Motoki S, Adachi J, Hikosaka Y, Ito K, Sano M, Soejima K, Yagishita A, Raseev G and Cherepkov N A 2000 *J. Phys. B: At. Mol. Opt. Phys.* **33** 4193
[6] Weber Th *et al* 2001 *J. Phys. B: At. Mol. Opt. Phys.* **34** 3669
[7] Jahnke T *et al* 2002 *Phys. Rev. Lett.* **88** 073002
[8] Dehmer J L and Dill D 1975 *Phys. Rev. Lett.* **35** 213
[9] Cherepkov N A, Raseev G, Adachi J, Hikosaka Y, Ito K, Motoki S, Sano M, Soejima K and Yagishita A 2000 *J. Phys. B: At. Mol. Opt. Phys.* **33** 4213
[10] Watanabe N, Adachi J, Soejima K, Shigemasa K and Yagishita A 1997 *Phys. Rev. Lett.* **78** 4910
[11] Wiley W C and McLaren I H 1955 *Rev. Sci. Instrum.* **26** 1150
[12] See http://roentdek.com for details on the detectors
[13] Tanaka T and Kitamura H 1996 *J. Synchrotron Radiat.* **3** 47
[14] Ohashi H, Ishiguro E, Tamenori Y, Kishimoto H, Tanaka M, Irie M and Ishikawa T 2001 *Nucl. Instrum. Methods* A **467/468** 529
[15] Ohashi H *et al* 2001 *Nucl. Instrum. Methods* A **467/468** 533
[16] Bozek J D, Saito N and Suzuki I H 1995 *Phys. Rev.* A **51** 4563
[17] Prince K C, Avaldi M, Coreno M, Camilloni R and de Simone M 1999 *J. Phys. B: At. Mol. Opt. Phys.* **32** 2551
[18] Slater J C 1974 *The Self-Consistent Field for Molecules and Solids: Quantum Theory of Molecules and Solids* vol 4 (New York: McGraw-Hill)